

A Benchmark System for Hardware-in-the-Loop Testing of Distributed Energy Resources

IEEE PES Task Force on Real-Time Simulation of Power and Energy Systems

PANOS KOTSAMPOPOULOS¹ (Member, IEEE), DIMITRIS LAGOS¹ (Member, IEEE),
 NIKOS HATZIARGYRIOU¹ (Fellow, IEEE), M. OMAR FARUQUE² (Senior Member, IEEE),
 GEORG LAUSS³ (Member, IEEE), ONYI NZIMAKO⁴ (Member, IEEE),
 PAUL FORSYTH⁴ (Member, IEEE), MICHAEL STEURER² (Senior Member, IEEE),
 F. PONCI⁵ (Member, IEEE), A. MONTI⁵ (Senior Member, IEEE),
 V. DINAHAHI⁶ (Senior Member, IEEE), AND KAI STRUNZ⁷ (Senior Member, IEEE)

¹Smart Grids Research Unit, School of Electrical and Computer Engineering, National Technical University of Athens, 15780 Zografou, Greece

²Center for Advanced Power Systems, Department of Electrical and Computer Engineering, Florida State University, Tallahassee, FL 32310 USA

³Energy Department, Austrian Institute of Technology, 1210 Vienna, Austria

⁴RTDS Inc., Winnipeg, MB R3T 2E1, Canada

⁵Institute for Automation of Complex Power Systems, E.ON Energy Research Center, RWTH Aachen University, 52074 Aachen, Germany

⁶Department of Electrical and Computer Engineering, University of Alberta, Edmonton, AB T6G 2V4, Canada

⁷SENSE Lab, Berlin University of Technology, 10587 Berlin, Germany

CORRESPONDING AUTHOR: M. O. FARUQUE (faruque@caps.fsu.edu)

ABSTRACT In order to overcome challenges associated with the integration of distributed energy resources (DER) into state-of-the-art and future power grids, a common basis for testing using appropriate benchmark systems is required. Real-time hardware-in-the-loop (HIL) simulation has proven to be an advanced and efficient tool for the analysis and validation of electric power systems and DER components. However, a common methodology for HIL testing of DER along with the required set of reference systems has not yet been developed. This task-force paper proposes a benchmark system for HIL testing incorporating DER into the real-time simulation environment. A low-voltage benchmark system with detailed HIL setup is proposed for the testing of DER performance. The modeling of DER for real-time applications is discussed, and the detailed laboratory procedures and setups for both controller HIL (CHIL) and power HIL (PHIL) are provided. Results from CHIL simulation related to the centralized controls and experimental results of PHIL simulation related to local control on the benchmark system substantiate the suitability of the proposed real-time simulation approach.

INDEX TERMS Benchmark systems, distributed energy resources, hardware in the loop simulation, microgrid, reference networks, real-time simulation.

I. INTRODUCTION

The challenges for the widespread integration of distributed energy resources require advanced simulation methods as well as a common basis for testing. Real-time hardware-in-the-loop (HIL) simulation based testing has been recognized as an advanced method for the analysis and testing of power system phenomena and components. Realistic, yet flexible testing conditions for de-risking equipment are its salient benefits. The suitability of HIL testing for distributed energy

resources (DER) related studies has been demonstrated in several publications and reports [1]–[8]. However, benchmark systems providing a common basis for testing and facilitating the analysis of DER integration at distribution and transmission level are required.

A number of benchmark reference systems for power system digital simulation studies can be found in the literature. IEEE has published several test systems for both transmission and distribution level, such as the IEEE 13, 16, 34 and 70 bus

distribution systems [9]. In 2013, CIGRE published the report “Benchmark Systems for Network Integration of Renewable and Distributed Energy Resources” [10], which proposes test systems for high voltage (HV), medium voltage (MV) and low voltage (LV) networks for both North America and Europe. The CIGRE European LV distribution network benchmark was derived from [11], while the North American is presented also in [12]. These benchmark networks have been used in several technical publications. In [13], the CIGRE MV benchmark and the IEEE HV 12 bus system were tested together on a real-time simulation platform to study high photovoltaic (PV) penetration. A fault diagnosis study was performed in the CIGRE MV benchmark in [14]. The operating modes of the CIGRE benchmark LV microgrid were simulated in [15]. Additional benchmark-reference networks, such as MV networks for China [16] and India [17], have also been proposed in the literature.

The implementation of benchmark systems in a digital real-time simulator (DRTS) as required for HIL testing is not straightforward. Moreover, real-time HIL simulation still lacks reference networks, test procedures, and guidelines in order to adopt them for DER related studies. Resolving these issues can facilitate the adoption of HIL simulation for standardized testing. This paper aims to address these deficiencies by defining a comprehensive benchmark network and guidelines for real-time HIL testing and simulation of DER related studies.

The structure of the paper is as follows: Section II shows a benchmark distribution network used as the basis for the development of reference systems for real-time HIL testing of DER technologies. Moreover, key technical considerations to adopt benchmark distribution networks from non-real-time simulation to real-time simulation for DER studies and HIL testing are discussed. Section III proposes benchmark test setups for control HIL (CHIL) and power HIL (PHIL) testing with recommendations on the equipment and reference laboratory procedures. Section IV presents CHIL and PHIL simulation results on the proposed benchmark systems and Section V concludes the paper.

II. BENCHMARK NETWORKS AND REAL-TIME SIMULATION

The CIGRE European LV distribution networks is used as the basis for the development of benchmark systems for HIL testing of DER. Fig. 1 shows a benchmark LV feeder, derived from the CIGRE European LV distribution network, which incorporates currently popular DER technologies namely photovoltaics, a combined heat and power microturbine, wind turbines, fuel cells and energy storage [18].

This benchmark LV network maintains important technical characteristics of an actual utility grid permitting efficient modeling and simulation with the different DER technologies. Key technical considerations for adopting benchmark networks for real-time simulation are discussed below.

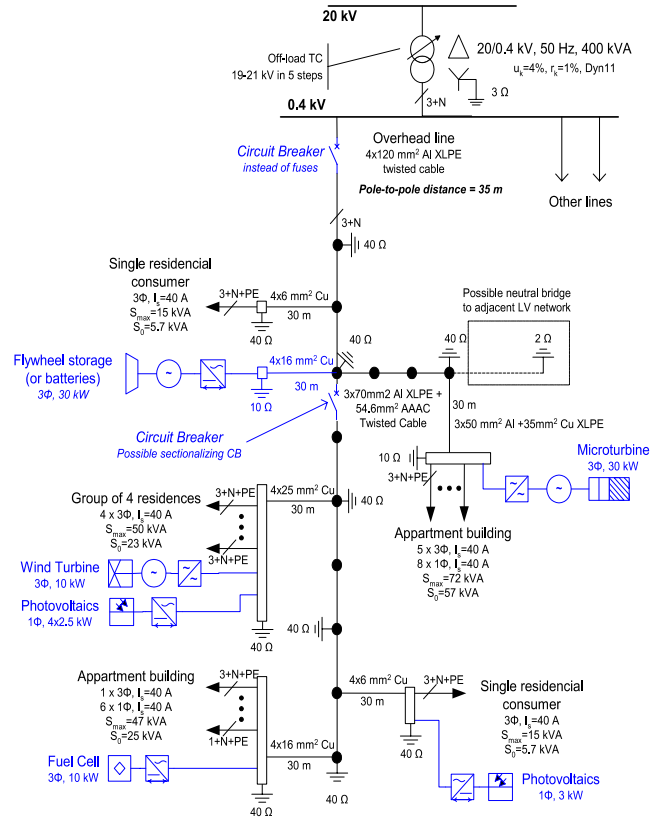


FIGURE 1. Benchmark LV network with DER based on the CIGRE network [18].

A. COMPUTATIONAL CAPABILITIES OF THE DRTS

DRTS compute the state of the modeled power system network at discrete time instances called the simulation time step. Time steps of approximately 50 μ s are typically used to simulate power system dynamic responses from DC to approximately 3 kHz. Smaller time steps ($<5 \mu$ s) are required to simulate higher frequency components and capture transients in DER power electronic converters stemming from power electronic switching events. Specialized methods such as adaptive discretization are available to preserve accuracy at larger time steps [19]. In order to achieve real-time simulation at the specified time step, the DRTS utilizes high-speed digital processors in a parallel architecture. The computational capabilities of the DRTS impose limitations on the network size, the number, and level of details of DER models and overall controls to be simulated within the specified time step [20].

In order to simulate large power system networks while maintaining the required simulation time step, parallel operation of different racks or computational units of the DRTS may be necessary. Large networks can be decoupled into subnetworks, which are solved independently and exchange boundary information with other racks/units at every time step. The subnetworks are usually decoupled using power systems network components such as transmission lines and cables with propagation times greater than the simulation

time step. Traveling wave models of overhead transmission lines and cables with lengths of 15 km and 5 km, respectively, exhibit a propagation delay greater than $50 \mu\text{s}$, which is the one time-step delay, typically seen between the parallel processing units. Shorter lines and cables, with lengths of 0.6 km and 0.2 km will have a propagation delay greater than $2 \mu\text{s}$ [21].

Such a decoupling technique becomes challenging in modeling distribution networks characterized by tightly coupled feeders having short lines and/or cables with propagation times less than the required time step. Artificially increasing the length of the line or cable, introduces large capacitance and unacceptable results such as bus voltages becoming unusually high [22]. In turn, using smaller time steps reduces the size of the distribution network and the scope of the study that can be simulated on the DRTS. Partition-based nodal solvers that reduce node count without adding delays have been reported in the literature and could extend to a certain point the size of the networks under study [23].

For a DRTS with limited computing capabilities, a reduced version of the network can be an acceptable option. For example, modeling a large system, such as the entire network of the CIGRE benchmark system including the full models of the DER primary sources and power electronic components, requires larger DRTS with state-of-the-art computing capabilities. If symmetric operating conditions are assumed, the single-phase equivalent can be employed to reduce the computational burden for simulating the network. In addition, the separation of the network in software (simulation in the DRTS) and actual hardware (DER, line(s), load(s), etc.) can further decrease the number of network nodes requiring explicit modeling [1].

B. LEVEL OF DETAILS IN THE DER MODELS

Another important factor for the real-time implementation is the level of details of DER models required for the study and HIL testing. Detailed component models of the DERs provide accurate modeling of the dynamics for the test applications but require increased computational resources in the DRTS. DER units can be represented in different ways, such as P-Q source models (including time constants, limiters etc) versus detailed dynamic models of each primary generator (e.g. wind turbine, PV panel, microturbine, etc), average models of converters versus full scale PWM models (e.g., for harmonics and dynamic overvoltage studies).

Fig. 2a shows a 6-pulse voltage source converter and Fig. 2b shows the average model of the voltage source converter. The average model neglects the switching frequency components allowing simulations at larger simulation time steps and hence reduced computational requirements. An alternative approach is the use of sub-cycle average models, which is a hybrid method between fully switched and average models [24]. The most appropriate option for each application is determined by the purpose of the studies and the capability of the available DRTS.

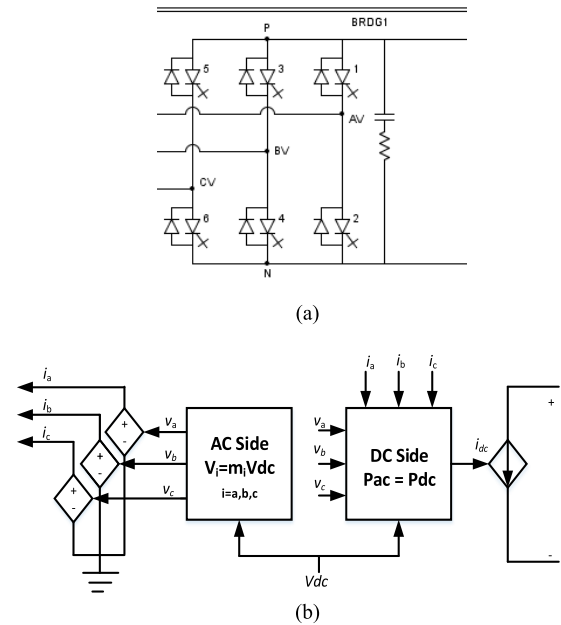


FIGURE 2. (a) Circuit diagram of a switched mode voltage source converter. (b) Average model of voltage source converter.

It should be noted that DRTS technologies continuously improve to allow modeling of increasingly higher frequency PWM switching phenomena. For example, FPGAs have been extensively used for detailed device-level modeling of fast switching power electronic apparatus used in AC and DC applications [25]–[27]. However, such capabilities may not be readily available in all locations where HIL testing takes place. Future efforts of this Task Force will focus on investigating general modeling approaches for real-time simulation systems.

III. DESCRIPTION OF BENCHMARK SETUP FOR HIL TESTING

In this section, a benchmark system is defined for HIL testing of DER. In order to define a benchmark setup/architecture for CHIL and PHIL testing, several aspects have to be considered, such as the requirements for the equipment, standard laboratory procedures, interfacing methods etc. In this way, the future use of CHIL and PHIL simulation in standardized testing of DER can be facilitated.

A. EQUIPMENT REQUIREMENTS

As mentioned in section II, the DRTS must demonstrate an acceptable time step to reproduce the dynamic behavior of interest within the simulated system in real-time. Fig. 3 shows the two classes of real-time HIL testing. Signals, such as voltages, currents and set points, are exchanged over the interface between the power system simulated in the real-time software of the DRTS and the physical device under test.

The signals can be either analog or digital depending on the nature of the interface. Amplifiers are required in the interface when the DRTS sends signals at levels lower than the

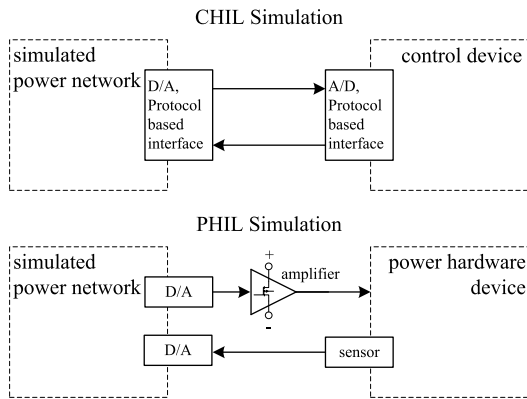


FIGURE 3. Basic approaches of CHIL and PHIL testing.

ratings of the device under test. The DRTS should comprise a sufficient number of accurate and fast input/output (I/O) devices and ideally a user-friendly graphical software interface to facilitate the HIL application. Apart from commercial solutions as described in [20], customized DRTS are used in some laboratories highlighting the need for requirements.

In CHIL simulation, a hardware controller is tested and linked to a power network simulated entirely in the real-time software of the DRTS. A typical application is the testing of an inverter controller implemented in a Digital Signal Processor (DSP), where the DSP sends set-points to the DRTS as digital signals and receives voltage and current measurements as analog signals from the DRTS. When testing a power system controller (e.g. microgrid controllers), the signal exchange between the controller and the DRTS can be performed via Ethernet based communication protocols. Therefore, the DRTS should provide appropriate analog and digital I/Os, as well as proper digital communication protocol interfaces. The design of the interface between the DRTS and the control equipment under test in CHIL applications is usually more straightforward than in PHIL simulation, as in many cases, the device ratings use low-level signals or Ethernet communication, which do not require any amplification or power transfer between the controller and the DRTS.

In PHIL simulation, the hardware under test (HUT) is a power component (e.g. a power electronic converter) therefore appropriate power amplification is necessary. Fig. 4 shows a PHIL test interface of a photovoltaic converter where the AC bus voltage from the simulated network in the DRTS is interfaced to the PV inverter through a D/A converter and power amplifier. The measured inverter current from the amplifier is fed back to the DRTS using an A/D converter to close the loop.

Due to the non-ideal power interface, additional stability and accuracy considerations are required for PHIL simulation. Crucial factors for stability are the loop delays inherent in the PHIL interface when exchanging signals between the DRTS and the power device under test. Large simulation time steps in the DRTS increase the total loop delay, which in

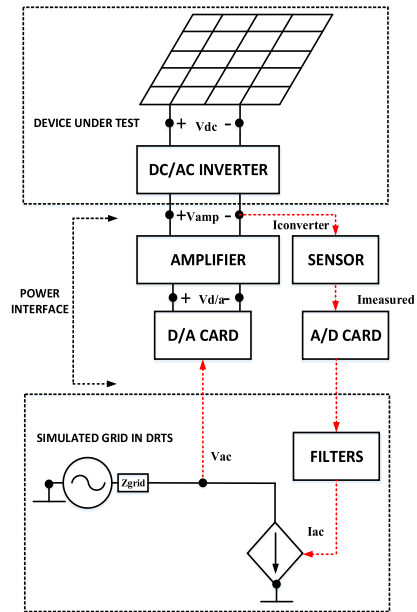


FIGURE 4. PHIL testing of a PV inverter.

principle increases the potential for instability in PHIL simulation. Moreover, filters in the power interface may impact stability and accuracy of the experiment.

The power amplifier should be able to receive and amplify signals from the DRTS with adequate signal accuracy, small time delay, sufficient frequency bandwidth, and low signal noise. Power amplifiers are mainly categorized as linear (LN) and switched mode (SM) devices. A comparative description of these technologies at PHIL simulations has been performed in [28]. Classification of overall simulation accuracy and bandwidth depends on the implemented case study. Transient investigations are performed in the range of 2 – 5 kHz, while power flow analysis is done in the range of 0.05 – 1 kHz. Based on this classification, the HIL equipment consisting of the power amplifier, DRTS, sensors, I/O and D/A, A/D converters can be selected and minimum requirements can be formulated.

As characteristics of each type of power amplifier (LN and SM) can differ significantly with respect to dynamic performance, it is suggested to put attention on specific requirements for each type. Indicative values for signal response times, slew rate, and amplification bandwidth are given in datasheets and have to be respected for voltage and current amplifiers used in the PHIL simulation setups.

B. REFERENCE LABORATORY PROCEDURES

The reference laboratory procedure for performing CHIL tests is proposed in Table 1. Table 2 shows the proposed reference laboratory procedure for PHIL tests. Variations of these procedures can be found in different laboratories, due to the differences of amplification units, protection strategies etc.

TABLE 1. Reference laboratory CHIL test procedure.

Step	Preparation of the experiment
I) Test case development	<ul style="list-style-type: none"> • Test case development (power system design, control algorithm design). • Modeling phase (implementation of real-time models and control algorithms on the DRTS, verification of real-time capability). • Classical digital simulation with fixed time delays between the control algorithm and the power system in the DRTS with emulated time delays.
II) Establishment of physical connections and accuracy evaluation	<ul style="list-style-type: none"> • Establishment of physical connections between the control board (hardware) and the I/O ports of the DRTS. • Full validation and calibration of interchanging signal paths.
Step	Execution of the experiment
III) Execution of the DRTS model	The simulated power system modeled in the DRTS is compiled and executed for continuous real-time simulation. The initiated execution implies DRTS output signals as inputs for the HUT.
IV) Algorithm upload on the HUT and measurements evaluation	The control algorithm is uploaded and compiled in the HUT. The signals provided by the DRTS are cross-checked in the HUT and the correct function is evaluated by subsequent measurements.
V) Control algorithm application	The control algorithm in the HUT is enabled, thus control signals are instantly produced and transferred to the DRTS.
VI) Control signals evaluation	All control signals are monitored and verified by means of a specific real-time monitoring interface within the DRTS.
VII) Obtaining the results	Results can be obtained in the following ways: <ul style="list-style-type: none"> • Hardware measurements • Software tools from the DRTS • Signal test points can be read out of the DRTS via available I/O ports and sent to an oscilloscope • Other Software

C. INTERFACING CONSIDERATIONS

Different interface algorithms for performing PHIL simulations have been proposed in [33]. Each approach presents several advantages and limitations mainly regarding the stability and accuracy. In practice, the Ideal Transformer Model (ITM) and the Damping Impedance Method (DIM) are the most commonly used interface algorithms. A recent review on this topic is performed in [34] along with a state-of-the-art status of PHIL simulation. Investigations on the accuracy of PHIL simulation are performed using the guidelines proposed in [29], [30], and [35]. Future work could aim to formalize the effect of different sources of error and uncertainty on the HIL accuracy and eventually equip the HIL test results with objective quality indicators.

IV. BENCHMARK HIL TEST RESULTS

A. CHIL RESULTS: CENTRALIZED CONTROL

The LV microgrid of Fig. 1 is implemented in the DRTS, as shown in Fig. 5. The following simplifications are made to facilitate the real-time simulations: single-phase equivalent representation and all the distributed generation (DG) units are considered to be PV systems modeled as P-Q sources.

TABLE 2. Reference laboratory PHIL test procedure.

Step	Preparation of the experiment
I) Test case development	<ul style="list-style-type: none"> • Test case development (power system configuration, characteristics of the network). • Modeling phase (implementation of real-time models and control algorithms on the DRTS, verification of real-time capability). • Providing sufficient level of protection by observing experimental quantities to bring the PHIL experiment to a safe state if unexpected behavior (HUT failure, instability, etc.) occurs
II) Stability and accuracy evaluation	<p>There are mainly two straightforward methods for evaluating the stability of a PHIL simulation system:</p> <ul style="list-style-type: none"> • Application of the Nyquist criterion on the open-loop transfer function of the closed-loop system derived from the block diagram representing the quasi-continuous model of the PHIL control system. • Dynamic simulation as a virtual emulation of the PHIL system, which contains all the parts and interactions of the PHIL experiment (real-time model, HUT, I/O, interface algorithm (IA)). <p>Accuracy evaluation is recommended based on methods described in [29][30] and the aforementioned virtual emulation of PHIL systems.</p>
III) Checking protection and compensation blocks	<ul style="list-style-type: none"> • In case a HUT (or power interface) is not known in certain detail, stability evaluation according to II) cannot ensure safe PHIL simulation operation. Therefore, the incorporation of protection schemes on the software side (safety routines in the DRTS) and on the hardware side (current, voltage, power, temperature, or control protection) is of key importance. Before the implementation of each PHIL test, the effective operation of the protection schemes should be fully verified. • In many occasions, stability-accuracy analysis has shown the need to use interface compensation measures [31], such as filtering on the feedback signals [32], in order to guarantee system stability of the PHIL test and/or improve accuracy. It is important to verify that the selected functions are enabled for the execution of the PHIL experiment.
Step	Execution of the experiment
IV) Execution of the DRTS model	The simulated system modeled in the software of the DRTS is compiled and executed in the following. While the model runs, it produces a low-voltage reference signal for the power interface that drives the PHIL simulation.
V) Power interface (PI) start-up	The PI produces an AC (or DC) voltage (or current) according to the set-point provided by the DRTS. It is recommended to check in advance the waveform and RMS value of the reference signal. Depending on the amplifier the start-up can be straightforward or may require several steps (e.g. connection to the utility grid, loading the DC bus, etc).
VI) Connection of the HUT with the power interface	The AC voltage produced by the power interface is applied to the HUT. The HUT can be connected with the power interface via a relay controlled by power interface software, thus power connection to the HUT is established.
VII) Sending the feedback signal from the power interface to the DRTS	Currents or voltages of the HUT are measured by embedded or external sensors of the PI. The measured signal is given as feedback to the DRTS after being properly scaled down (if necessary), in order not to exceed its input limits.
VIII) Closing the loop	This procedure is performed in the software of the DRTS by closing a switch. It is recommended to check in advance the validity of the feedback signal.
IX) Obtaining the results	<ul style="list-style-type: none"> • Similar to CHIL setup

The daily load curves of the benchmark microgrid, as proposed in [18], and a typical irradiation profile of a sunny day are used.

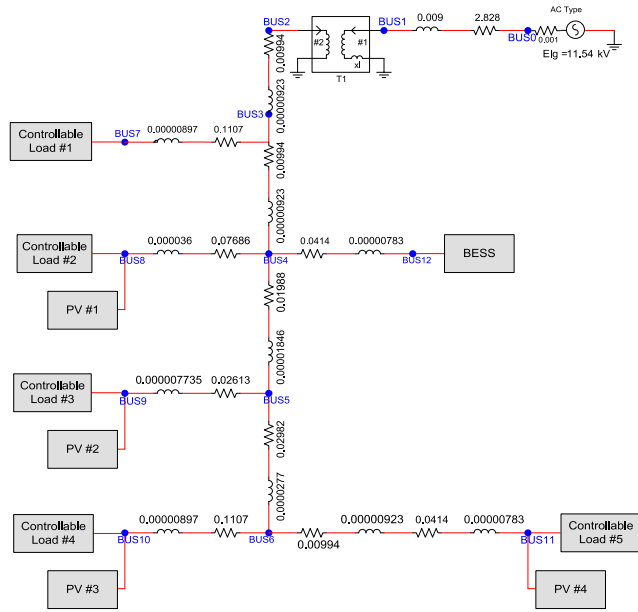


FIGURE 5. The simplified version of the benchmark LV microgrid simulated in the DRTS software.

A centralized control scheme is applied to perform peak shaving in combination with optimal coordinated voltage control. The optimization algorithm aims to minimize the node voltage deviations and active power losses on the distribution lines and transformer. The method is an extension of the algorithm developed in [36]. The control algorithm is implemented on a hardware controller and is tested at a CHIL test setup as shown in Fig. 6.

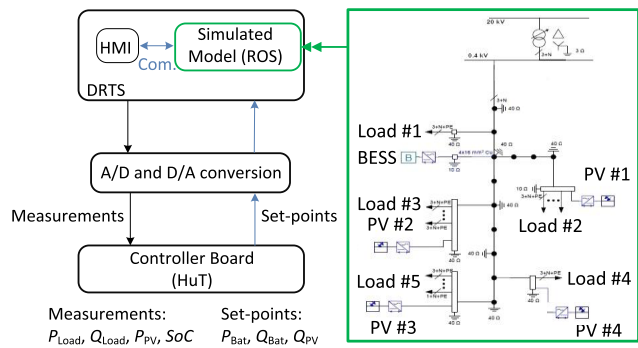


FIGURE 6. CHIL test setup of the benchmark system.

The active power exchange between the main grid and the microgrid is measured at the secondary of the MV/LV transformer. The results with and without the implementation of the centralized control are presented in Fig. 7. At high irradiation, active power flows from the microgrid to the upstream network, as the DG's production exceeds the load.

The peak shaving operation is shown clearly during peak load at a time interval $t \in [18:00 \text{ h}; 22:30 \text{ h}]$, when the battery storage system provides active power, as highlighted in Fig. 8.

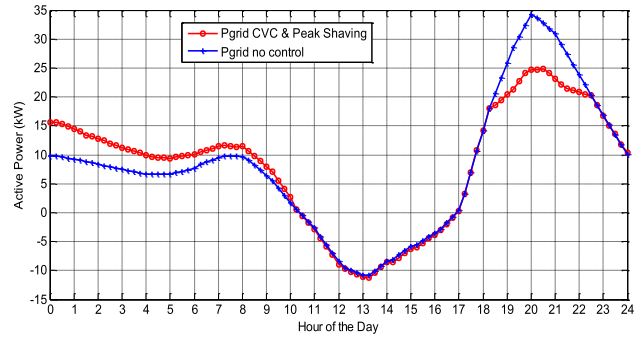


FIGURE 7. Active power exchange between the main grid and the microgrid with and without the centralized control (CHIL simulation).

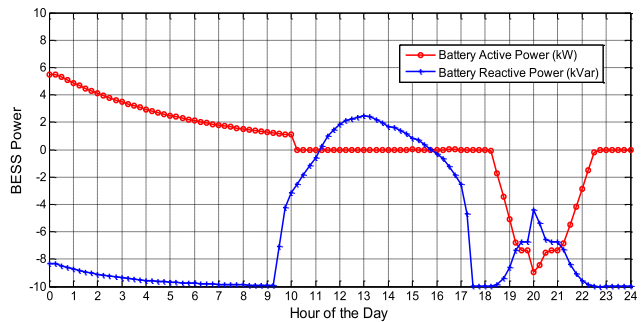


FIGURE 8. Active and reactive power of the storage system (CHIL simulation).

During low load conditions, the storage system absorbs active power to reach a target state of charge. The reactive power of the storage system helps to support the voltage and the active and reactive power as well as the state of charge of the storage system are shown in Fig. 8 and Fig. 9, respectively.

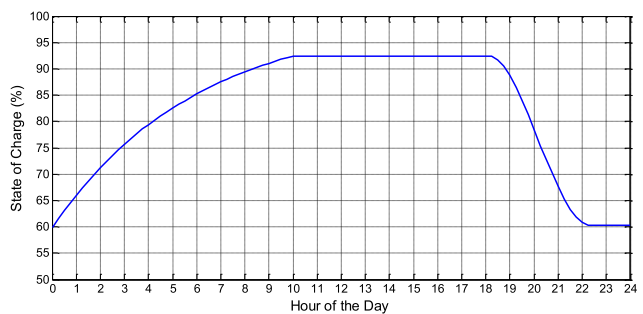


FIGURE 9. State of charge of the storage system (CHIL simulation).

The reactive power of the PV systems during the CHIL simulation is depicted in Fig. 10. Fig. 11 and Fig. 12 show that the operation of the centralized control algorithm manages also to improve the node voltages of the benchmark system. In this way, the operation of the developed controller is tested conveniently under realistic conditions in the lab, before field deployment.

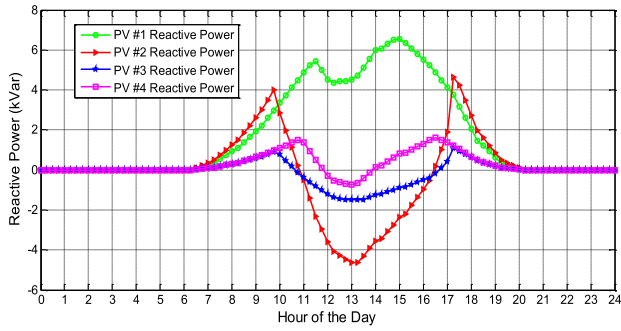


FIGURE 10. Reactive power of PV systems (CHIL simulation).

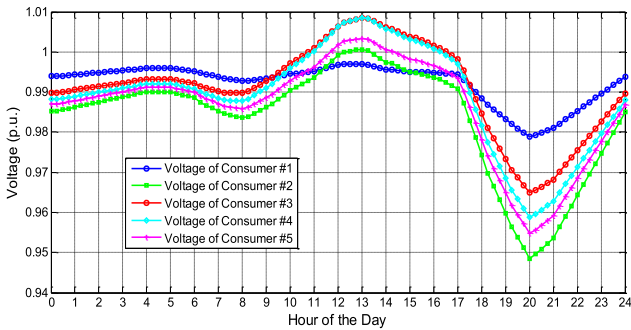


FIGURE 11. Node voltages without the operation of the centralized control algorithm (CHIL simulation).

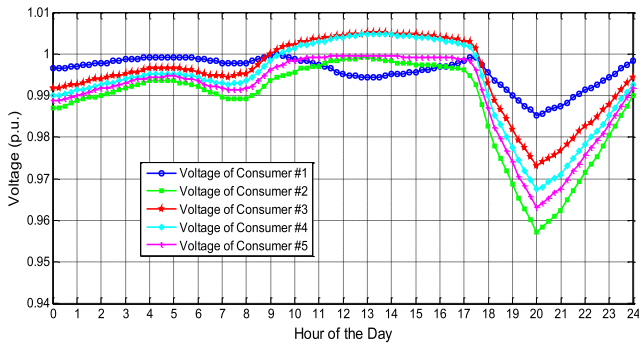


FIGURE 12. Node voltages during the operation of the centralized control algorithm (CHIL simulation).

B. PHIL RESULTS: LOCAL CONTROL

The aforementioned benchmark LV microgrid of Fig. 1 is implemented in the DRTS, as depicted in Fig. 5 and is tested in both grid-connected and islanded operation using the PHIL simulation methodology.

1) GRID-CONNECTED MICROGRID OPERATION

The following simplifications were made to facilitate the real-time simulations: single-phase equivalent representation and all the DG units are considered to be PV systems modeled as P-Q sources. A commercial PV inverter with a rated single phase AC power of 3 kVA and advanced ancillary services capabilities is used as the HUT. It is connected to the bus of load#4 via a suitable power interface consisting of a linear

amplifier and a current sensor. The PHIL simulation setup including the simulation of the benchmark system is shown in Fig. 13.

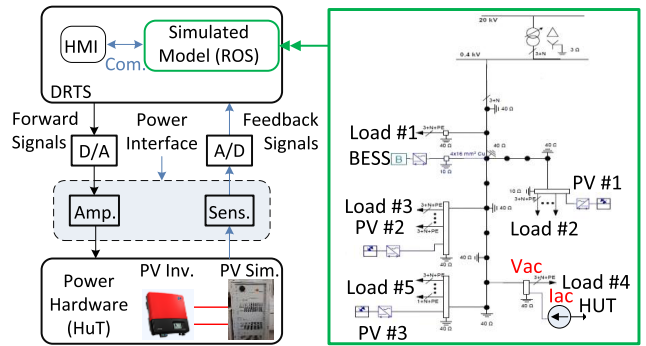


FIGURE 13. PHIL test setup of the benchmark system.

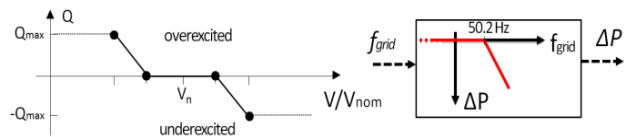


FIGURE 14. Typical $Q(U)$ and $P(f)$ droop characteristics incorporated in the inverters of DG units according to recent standards.

The simulated and hardware DG units provide voltage and frequency support, according to recent standards [37], by employing the $Q(U)$ and $P(f)$ droop characteristics shown in Fig. 14. At a time of high irradiation, the total load of the microgrid is reduced. The load values are chosen from the daily load curves of the benchmark microgrid according to [18]. The node voltages with and without the operation of the $Q(U)$ droop controllers of the DGs during the PHIL test are shown in Fig. 15. The reactive power absorption results in voltages closer to the nominal value. As the hardware PV inverter operates near its nominal operating point, it reduces its active power to absorb reactive power, according to the $Q(U)$ characteristic, in order to respect the apparent power limitation. As a result, some fluctuations occur on the

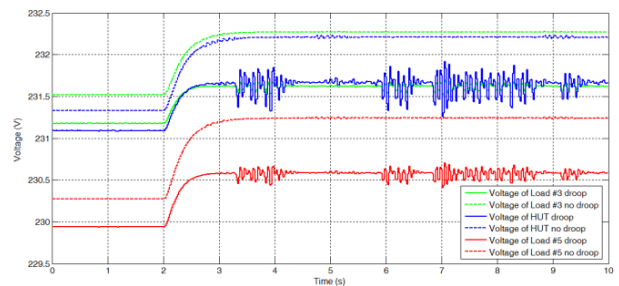


FIGURE 15. Node voltages with and without the operation of the $Q(U)$ droop controllers of the DGs (PHIL simulation).

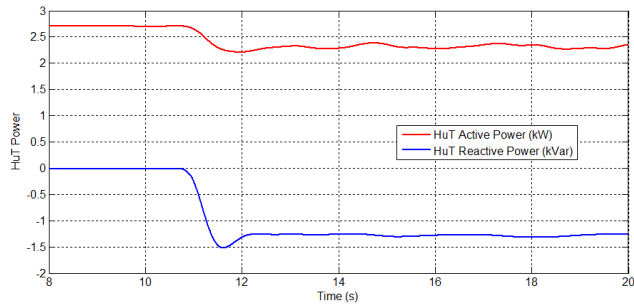


FIGURE 16. Active and reactive power of the hardware PV inverter: active power reduction to absorb reactive power according to the $Q(U)$ droop (PHIL simulation).

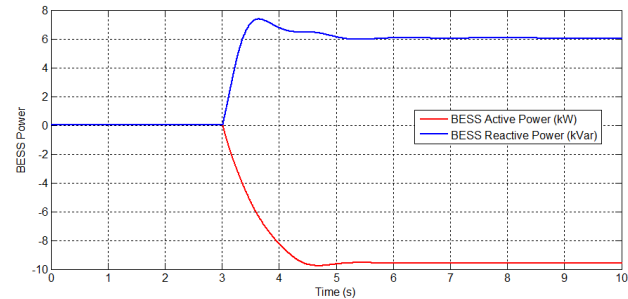


FIGURE 17. Active and reactive power of the storage system at the transition from grid connected to island mode (PHIL simulation).

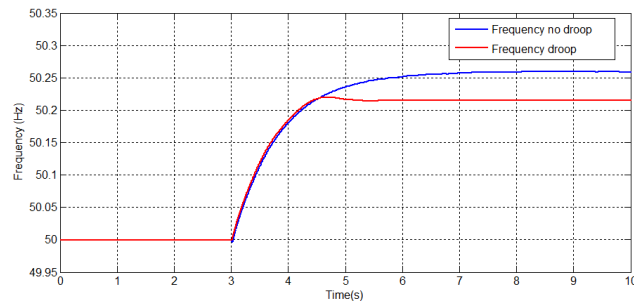


FIGURE 18. Microgrid frequency at the transition from grid connected to island mode: the $P(f)$ droop of the DGs lead to an improved frequency response (PHIL simulation).

voltages, which are illustrated in Fig. 15. This operation is made clearer in Fig. 16, where initially the $Q(U)$ controller is deactivated and receives the activation command.

2) ISLANDED MICROGRID OPERATION

The islanded operation of the benchmark microgrid is investigated, including the transition from grid connected to the islanded operation. The storage system employs the common $f(P)$, $V(Q)$ droop curves in island mode [15] and the DG units employ $P(f)$ and $Q(U)$ droop characteristics shown in Fig. 14.

PHIL tests are performed for the case of high irradiation. At the transition to islanded operation, the storage system

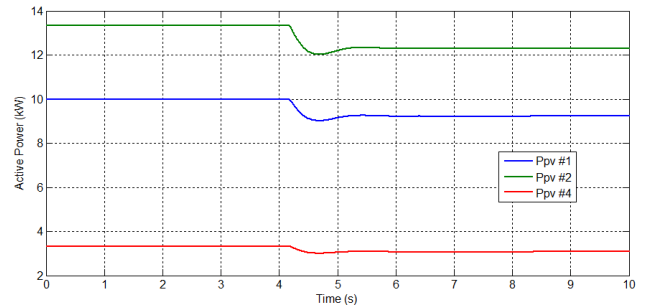


FIGURE 19. Active power curtail of the simulated DGs at the transition from grid connected to island mode (PHIL simulation).

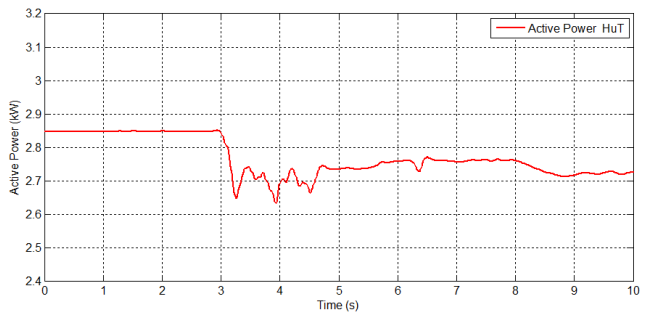


FIGURE 20. Active power curtail of the hardware PV inverter at the transition from grid connected to island mode (PHIL simulation).

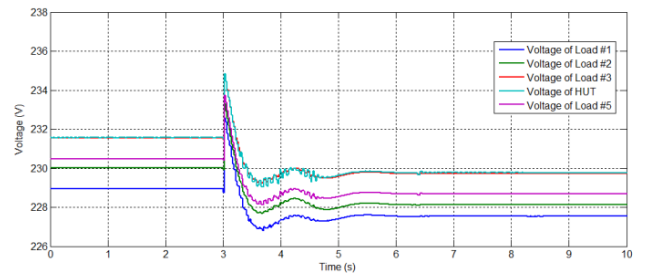


FIGURE 21. Node voltages at the transition from grid connected to island mode (PHIL simulation).

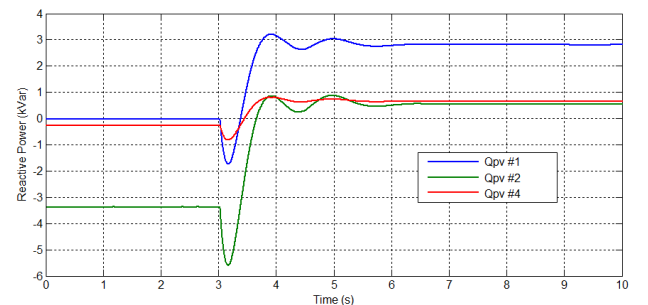


FIGURE 22. Reactive power of the simulated DGs at the transition from grid connected to island mode (PHIL simulation).

begins to absorb active power, due to the high DG production, and provides reactive power (Fig. 17). The microgrid frequency and voltages are mainly influenced by the droop curves of the storage system and the DGs. The high DG

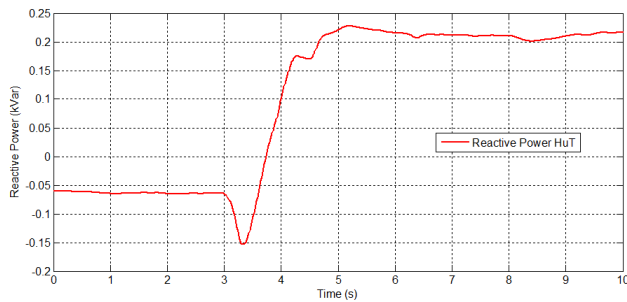


FIGURE 23. Reactive power of the hardware DG at the transition from grid connected to island mode (PHIL simulation).

production leads to an increase of the frequency as shown in Fig. 18, which is limited by the active power curtail droop characteristic of the DGs at over-frequency. The $P(f)$ droop control of the DGs leads to an improved frequency response, as illustrated in Fig. 18. The production of all the DGs is reduced at frequencies exceeding the 50.2 Hz threshold, as illustrated in Fig. 19 and 20 for the simulated and hardware DGs, respectively. Fig. 21 shows that the voltage reduction due to the reactive power demand (the storage system operates with a $V(Q)$ droop characteristic), is mitigated by the reactive power provision of the DGs, according to their $Q(U)$ characteristics. The reactive power of the simulated and hardware DGs is illustrated in Fig. 22 and 23, respectively.

V. CONCLUSION

The paper offers important insight into the HIL testing of power hardware and controllers of distributed energy resources in distribution networks. The main outcomes are as follows:

a) Established benchmark systems for analytical studies are selected and the applicability and real-time capability for relevant studies are addressed.

b) Reference test procedures for real-time simulation methods such as CHIL and PHIL are elaborated. The focus is on the provision of practical guidelines, which can help researchers to set up HIL simulations in a laboratory environment in a structured and safe way.

c) Two advanced test cases applying the proposed HIL methodologies are reported. At the CHIL benchmark system, a hardware central controller executing an optimization algorithm is tested. Peak shaving, voltage control and minimization of losses are evaluated in realistic conditions. Local control of the DER units is evaluated at the PHIL benchmark system at both grid-connected and islanded operation. The impact of the hardware PV inverter on the voltage regulation is shown at grid-connected operation. The performance of standard droop control functions of PV inverters for grid-connected operation is investigated during the transition to islanded operation

ACKNOWLEDGMENT

The authors would like to acknowledge the help of members of the IEEE PES Task Force on Real-Time

Simulation of Power and Energy Systems, Ali Davoudi, University of Texas-Arlington, USA, Beat Arnet, Plexim, USA, Andrea Benigni, University of South Carolina, USA, Harikrishna Mada, Indian Institute of Technology Roorkee, India, Christian Dufour, OPAL-RT, Canada in preparation of this paper.

REFERENCES

- [1] P. C. Kotsampopoulos, F. Lehfuß, G. F. Lauss, B. Bletterie, and N. D. Hatzigiorgiou, "The limitations of digital simulation and the advantages of PHIL testing in studying distributed generation provision of ancillary services," *IEEE Trans. Ind. Electron.*, vol. 62, no. 9, pp. 5502–5515, Sep. 2015.
- [2] J. Wang, Y. Song, W. Li, J. Guo, and A. Monti, "Development of a universal platform for hardware in-the-loop testing of microgrids," *IEEE Trans. Informat.*, vol. 10, no. 4, pp. 2154–2165, Nov. 2014.
- [3] C. Molitor *et al.*, "Multiphysics test bed for renewable energy systems in smart homes," *IEEE Trans. Ind. Electron.*, vol. 60, no. 3, pp. 1235–1248, Mar. 2013.
- [4] V. Karapanos, S. de Haan, and K. Zwetsloot, "Real time simulation of a power system with VSG hardware in the loop," in *Proc. IEEE 37th Annu. IES Conf. IECON*, Melbourne, VIC, Australia, Nov. 2011, pp. 3748–3754.
- [5] G. Lauss, F. Lehfuß, B. Bletterie, T. Strasser, and R. Bründlinger, "Examination of LV grid phenomena by means of PHIL testing," in *Proc. IEEE 38th Annu. IES IECON Conf.*, Montreal, QC, Canada, Oct. 2012, pp. 4771–4776.
- [6] B. Palmintier, B. Lundstrom, S. Chakraborty, T. Williams, K. Schneider, and D. Chassin, "A power hardware-in-the-loop platform with remote distribution circuit cosimulation," *IEEE Trans. Ind. Electron.*, vol. 62, no. 4, pp. 2236–2245, Apr. 2015.
- [7] Y. Zhou, H. Li, and L. Liu, "Integrated autonomous voltage regulation and islanding detection for high penetration PV applications," *IEEE Trans. Power Electron.*, vol. 28, no. 6, pp. 2826–2841, Jun. 2013.
- [8] P. C. Kotsampopoulos, V. A. Kleftakis, and N. D. Hatzigiorgiou, "Laboratory education of modern power systems using PHIL simulation," *IEEE Trans. Power Syst.*, vol. 32, no. 5, pp. 3992–4001, Sep. 2017.
- [9] C. Lee, C. Liu, S. Mehrotra, and Z. Bie, "Robust distribution network reconfiguration," *IEEE Trans. Smart Grid*, vol. 6, no. 2, pp. 836–842, Mar. 2015.
- [10] *CIGRE Task Force C6.04.02: Benchmark Systems for Network Integration of Renewable and Distributed Energy Resources*, CIGRE, Paris, France, May 2013.
- [11] *Advanced Architectures and Control Concepts for More Microgrids*, More Microgrids, EU Commission, Brussels, Belgium, 2009.
- [12] K. Strunz, R. H. Fletcher, R. Campbell, and F. Gao, "Developing benchmark models for low-voltage distribution feeders," in *Proc. IEEE Power Eng. Soc. Gen. Meeting*, Calgary, AB, Canada, Jul. 2009, pp. 1–3.
- [13] B.-I. Crăciun, T. Kerekes, D. Séra, R. Teodorescu, and A. Timbus, "Benchmark networks for grid integration impact studies of large PV plants," in *Proc. IEEE Grenoble Conf. Aalborg*, Denmark: Aalborg Univ., Jun. 2013, pp. 1–6.
- [14] A. M. El-Zonkoly, "Fault diagnosis in distribution networks with distributed generation," *Electr. Power Syst. Res.*, vol. 81, no. 7, pp. 1482–1490, Jul. 2011.
- [15] N. L. Soutanis, S. A. Papanthasiou, and N. D. Hatzigiorgiou, "A stability algorithm for the dynamic analysis of inverter dominated unbalanced LV microgrids," *IEEE Trans. Power Syst.*, vol. 22, no. 1, pp. 294–304, Feb. 2007.
- [16] Y. Fan, F. Ming-Tian, and Z. Zu-Ping, "China MV distribution network benchmark for network integrated of renewable and distributed energy resources," in *Proc. China Int. Conf. Electr. Distrib. (CICED)*, Nanjing, China, 2010, pp. 1–7.
- [17] R. Bhakar, N. P. Padhy, and H. O. Gupta, "Reference network development for distribution network pricing," in *Proc. IEEE PES Transmiss. Distrib. Conf. Expo.*, New Orleans, LA, USA, Apr. 2010, pp. 1–8.
- [18] S. Papanthasiou, N. Hatzigiorgiou, and K. Strunz, "A benchmark low voltage microgrid network," in *Proc. CIGRE Symp. Power Syst. Dispersed Gener.*, Athens, Greece, Apr. 2005, p. 313.
- [19] M. O. Faruque and V. Dinavahi, "Hardware-in-the-loop simulation of power electronic systems using adaptive discretization," *IEEE Trans. Ind. Electron.*, vol. 57, no. 4, pp. 1146–1158, Apr. 2010.

- [20] M. D. O. Faruque *et al.*, “Real-time simulation technologies for power systems design, testing, and analysis,” *IEEE Power Energy Technol. Syst. J.*, vol. 2, no. 2, pp. 63–73, Jun. 2015.
- [21] P. Forsyth, O. Nzimako, C. Peters, and M. Moustafa, “Challenges of modeling electrical distribution networks in real-time,” in *Proc. Int. Symp. Smart Electr. Distrib. Syst. Technol. (EDST)*, Vienna, Austria, 2015, pp. 556–559.
- [22] M. Dyck and O. Nzimako, “Real-time simulation of large distribution networks with distributed energy resources,” in *Proc. 24th Int. Conf. Exhib. (CIRED)*, 2017, pp. 1402–1405.
- [23] H. Hooshyar, L. Vanfretti, and C. Dufour, “Delay-free parallelization for real-time simulation of a large active distribution grid model,” in *Proc. 42nd Annu. Conf. IEEE Ind. Electron. Soc. (IECON)*, Florence, Italy, 2016, pp. 6278–6284.
- [24] J. Allmeling and N. Felderer, “Sub-cycle average models with integrated diodes for real-time simulation of power converters,” in *Proc. 3rd IEEE Southern Power Electron. Conf.*, Puerto Varas, Chile, Dec. 2017, pp. 1–6.
- [25] A. Myaing and V. Dinavahi, “FPGA-based real-time emulation of power electronic systems with detailed representation of device characteristics,” *IEEE Trans. Ind. Electron.*, vol. 58, no. 1, pp. 358–368, Jan. 2011.
- [26] O. Jiménez, O. Lucía, I. Urriza, L. A. Barragan, D. Navarro, and V. Dinavahi, “Implementation of an FPGA-based online hardware-in-the-loop emulator using high-level synthesis tools for resonant power converters applied to induction heating appliances,” *IEEE Trans. Ind. Electron.*, vol. 62, no. 4, pp. 2206–2214, Apr. 2015.
- [27] Z. Shen and V. Dinavahi, “Real-time device-level transient electrothermal model for modular multilevel converter on FPGA,” *IEEE Trans. Power Electron.*, vol. 31, no. 2, pp. 6155–6168, Sep. 2016.
- [28] F. Lehfuß, G. Lauss, P. Kotsampopoulos, N. Hatzigiargyriou, P. Crolla, and A. Roscoe, “Comparison of multiple power amplification types for power hardware-in-the-loop applications,” in *Proc. IEEE Workshop Complex. Eng. (COMPENG)*, Aachen, Germany, Jun. 2012, pp. 1–6.
- [29] W. Ren, M. Steurer, and T. L. Baldwin, “An effective method for evaluating the accuracy of power hardware-in-the-loop simulations,” *IEEE Trans. Ind. Appl.*, vol. 45, no. 4, pp. 1484–1490, Jul. 2009.
- [30] A. Viehweider, G. Lauss, and L. Felix, “Stabilization of power hardware-in-the-loop simulations of electric energy systems,” *Simul. Model. Pract. Theory*, vol. 19, no. 7, pp. 1699–1708, Aug. 2011.
- [31] W. Ren *et al.*, “Interfacing issues in real-time digital simulators,” *IEEE Trans. Power Del.*, vol. 26, no. 2, pp. 1221–1230, Apr. 2011.
- [32] G. Lauss, F. Lehfuß, A. Viehweider, and T. Strasser, “Power hardware in the loop simulation with feedback current filtering for electric systems,” in *Proc. 37th Annu. Conf. IEEE Ind. Electron. Soc. (IECON)*, Melbourne, VIC, Australia, Nov. 2011, pp. 3725–3730.
- [33] W. Ren, M. Steurer, and T. L. Baldwin, “Improve the stability and the accuracy of power hardware-in-the-loop simulation by selecting appropriate interface algorithms,” *IEEE Trans. Ind. Appl.*, vol. 44, no. 4, pp. 1286–1294, Jul./Aug. 2008.
- [34] G. F. Lauss, M. O. Faruque, K. Schoder, C. Dufour, A. Viehweider, and J. Langston, “Characteristics and design of power hardware-in-the-loop simulations for electrical power systems,” *IEEE Trans. Ind. Electron.*, vol. 63, no. 1, pp. 406–417, Jan. 2016.
- [35] A. Riccobono, E. Liegmann, M. Pau, F. Ponci, and A. Monti, “Online parametric identification of power impedances to improve stability and accuracy of power hardware-in-the-loop simulations,” *IEEE Trans. Instrum. Meas.*, vol. 66, no. 9, pp. 2247–2257, Sep. 2017.
- [36] M. Maniatopoulos, D. Lagos, P. Kotsampopoulos, and N. Hatzigiargyriou, “Combined control and power hardware in-the-loop simulation for testing smart grid control algorithms,” *IET Gener., Transmiss. Distrib.*, vol. 11, no. 12, pp. 3009–3018, Aug. 2017.
- [37] P. Kotsampopoulos, N. Hatzigiargyriou, B. Bletterie, and G. Lauss, “Review, analysis and recommendations on recent guidelines for the provision of ancillary services by distributed generation,” in *Proc. IEEE Int. Workshop Intell. Energy Syst. (IWIES)*, Vienna, Austria, Nov. 2013, pp. 185–190.

Authors’ photographs and biographies not available at the time of publication.